Arabian Journal of Chemistry (2021) **14**, 103267

King Saud University

Arabian Journal of Chemistry

www.ksu.edu.sa
www.sciencedirect.com

ORIGINAL ARTICLE

Multifunctional magnetic bio-nanoporous carbon material based on zero-valent iron, Angelicae Dahuricae Radix slag and graphene oxide: An efficient adsorbent of pesticides

Hua Du [a], Yutian Lei [a], Wenli Chen [a], Fengchao Li [a], Huimin Li [a], Wei Deng [b], Guihua Jiang [a,b,*]

[a] *College of Pharmacy, Chengdu University of TCM, Sichuan 611137, China*
[b] *College of Ethnic Medicine, Chengdu University of TCM, Sichuan 611137, China*

Received 8 April 2021; accepted 12 June 2021
Available online 30 June 2021

KEYWORDS

Bio-nanocomposite;
Pesticide removal;
Sewage treatment;
Adsorption kinetics and isotherm;
Implicit mechanism

Abstract A low-cost and recyclable multifunctional adsorbent for pesticides was successfully prepared based on herb waste (Angelicae Dahuricae Radix slag), nano-zero-valent iron and graphene oxide (AS/NZVI/GO) via facile one-step pyrolysis approach, and applied to remove pesticides from sewage. The AS/NZVI/GO possesses some excellent merits which are beneficial to achieve high adsorption efficiency, including abundant pore structures, lots of surface functional groups and high specific surface area. The maximum adsorption capacity of AS/NZVI/GO for methomyl, isoprocarb and carbaryl up to 59.13, 21.33 and 61.91 $mg \cdot g^{-1}$, respectively, proved the good adsorption efficiency of AS/NZVI/GO for pesticides. The adsorption mechanism was mainly associated with pore filling, π-π electron-donor–acceptor interaction, hydrogen bonding and electrostatic interaction. The results showed that the pseudo-second-order kinetic model and Freundlich isotherm model showed a better correlation for the experiment data, indicating that the overall rate of the adsorption process was controlled mainly by physical and chemical adsorption. Furthermore, the reusability experiment exhibited that the removal efficiency of AS/NZVI/GO for three pesticides was more than 70% after five recycles. To sum up, it could conclude that the novel AS/NZVI/GO can be used as an efficient adsorbent for the removal of pesticides.

* Corresponding author at: College of Pharmacy, Chengdu University of TCM, Sichuan 611137, China.
E-mail address: 11469413@qq.com (G. Jiang).

Peer review under responsibility of King Saud University.

Production and hosting by Elsevier

https://doi.org/10.1016/j.arabjc.2021.103267
1878-5352

1. Introduction

Pesticides, one kind of effective insecticide, play an important role in improving the yield of crops and removing pests from crops, and have been widely used in agricultural fields (Zhou et al., 2018b). However, as the use of pesticides has greatly increased, a large amount of wastewater containing pesticide residues is discharged into rivers without treatment, or directly enters into the groundwater body, which not only leads to serious damage to the ecological environment and serious pollution of water resources but also may cause harm to humans, animals and plants (Alothman et al., 2020b). It was reported that the pesticide molecules might inhibit the activity of acetylcholinesterase and kill immune T cells, thereby make people suffer from cancer, teratogenesis, and mutation (Bucur et al., 2014). However, it is difficult to effectively remove those pesticides from wastewater by conventional sewage treatment methods. Therefore, it is of great importance to developing a low-cost and efficient method to remove pesticides in sewage.

Adsorption was considered as an effective method to remove pesticide residues or heavy metal residues, which has been widely adopted in various fields (Alothman et al., 2020a; Gu et al., 2020; Li et al., 2017; Markus et al., 2018; Yadav et al., 2019). The existing adsorbents mainly include some commercial or synthetic adsorbents, such as silica gel, alumina and polyamide. However, the chemically synthesized adsorbents have the disadvantages of being environmentally unfriendly and high cost. It is difficult to achieve large-scale applications. Therefore, it is of great significance to develop a low-cost and environmentally friendly adsorbent. Biochar, a product obtained by pyrolysis of biomass, has the advantages of low cost, porous structure, renewable and reusable properties, and environmental friendliness, and has considered being a high effect and low-cost adsorbent (Al-Marghany et al., 2021; Deng et al., 2020; Habila et al., 2018; Jiang et al., 2017; Olu-Owolabi et al., 2017; Shi et al., 2016; Shu et al., 2018; Subedi et al., 2019; Zhang et al., 2018b; Zhao et al., 2018). Thus, the adsorbent of biomass-based has been widely applied, especially the wasted biomass. Recently, with the rapid development of traditional Chinese medicine, a large amount of Chinese medicinal waste residues has remained. such as Angelicae Dahuricae Radix slag (AS), a Chinese medicine material used to treat migraine. The AS, a kind of wasted biomass, can be used as an ideal material for biochar preparation. The reason is that it is considered to be a good carbon precursor because of its high carbon content and easily activated components such as cellulose, lignin and hemicellulose, and it contains various kinds of chemical components such as alcohols, esters, alkaline and small amount of ketone etc., (Sun et al., 2018). In general, centrifugation and filtration methods are used to separate the adsorbent material from aqueous solution (Duman et al., 2016). These applications are time-consuming and require extra cost (Duman et al., 2019). Compared with traditional centrifugation and filtration methods, magnetic separation method is an efficient, fast and economic method for the separation of magnetic adsorbents from the medium after the adsorption treatment of pollutants is completed (Duman et al., 2017). The separation of non-magnetic adsorbents from sample solution after adsorption process is very difficult and also time-consuming. This problem can be solved by the incorporation of magnetic nanoparticles on the surfaces of nanocomposite adsorbents and then by using a magnet (Nouri et al., 2020; Sereshti et al., 2020). Furthermore, combining carbon materials with NZVI could effectively increase the dispersibility and stability of NZVI (Qi et al., 2020; Zhu et al., 2017; Zhu et al., 2009).

In addition, the adsorption efficiency of adsorbents could be significantly improved by combining organic and inorganic materials (Shi et al., 2016). Thus, in the current study, the biochar and organic graphene oxide were combined and applied to prepare the new material. Graphene oxide (GO), a derivative of graphene, is considered a multifunctional adsorbent which contains a lot of aromatic structure. The adsorbate can be adsorbed by forming π-π interaction with GO. At the same time, it has a large number of functional groups such as hydroxyl groups, carboxyl groups, and carbonyl groups. These functional groups can significantly improve the dispersibility of the adsorbent in water and significantly improve the adsorption efficiency (Zhang et al., 2019; Zubir et al., 2014). However, GO, as a commercial adsorbent, is difficult to achieve large-scale applications due to the shortcomings of high cost and environmental pollution. Thus, a combination of GO with biochar may solve this problem. That is, a small amount of GO is assembled on the surface of biochar to form a new composite material (Zhou et al., 2019). The new composite material may not only have the advantages of environmental friendliness, low price, multi-functional groups and aromaticity but also reveals unique structures and excellent adsorption performance.

In the present study, in order to efficiently and quickly remove pesticide residues in sewage, a novel magnetic bio-char nanoporous carbon material based on nano-zero-valent iron, Angelicae Dahuricae Radix slag and graphene oxide has been successfully prepared. Then the AS/NZVI/GO was characterized (SEM, BET, FTIR, XPS, Raman and VSM) and used for the adsorption of pesticide residues from sewage. The key factors influencing the adsorption efficiency, including pyrolysis temperature and amount of the GO added, pH of the initial solution and amount of adsorbent were studied. Meanwhile, the adsorption behavior of AS/NZVI/GO composite, including the adsorption kinetics, isotherms, mechanisms affecting the adsorption capacity was studied. Finally, AS/NZVI/GO exhibited high adsorption efficiency and reusability in the optimal condition.

2. Materials and methods

2.1. Materials, reagents and instrumentation

The waste biomass, Angelicae Dahuricae Radix slag (AS), was provided by the school of pharmacy, Chengdu University of Traditional Chinese Medicine. The graphene oxide powder (GO) was purchased from Jining Leader Nano Technology Co., Ltd (Shandong, China). The $FeCl_3{\cdot}6H_2O$, potassium hydroxide, sodium hydroxide, hydrochloric acid and ammonium acetate, analytical grade ethanol and formic acid were purchased from Beijing J & K Technology Co., Ltd. (Beijing, China). The acetonitrile was collected provided by Tedia, Fairfield, OH, USA. The standards of three pesticides, including methomyl, isoprocarb and carbaryl (analytic grade $\geq$ 99.0% purity), were purchased from Dr. Ehrenstorfer GmbH (Augsburg, Germany). The double-distilled water was prepared by Milli-Q-plus ultra-pure water system (Milford, MA, USA).

The experiment was carried out on the LC-30 ultra-high-performance liquid chromatography system (Shimadzu, Japan). API5500Q triple quadrupole linear ion trap mass spectrometer interface for electrospray (ESI) (AB Sciex, USA) was used for mass spectrometry detection. The multiple reactions monitoring mode (MRM) was used to monitor the analytes. UPLC separation was performed on a Waters ACQUITY UHPLC® BEH C18 column (100 mm × 2.1 mm i.d., 1.7 μm, Waters Corp., Milford, MA, USA). The analysis condition as follows: flow rate (0.3 mL min^{-1}), injection volume (2 μL), column temperature (40 ℃). The mobile phase includes acetonitrile (phase A) and 0.2 mmol L^{-1} ammonium acetate water contained 0.1% formic acid (phase B). The gradient system elution program as follows: 0–2 min, 90% B; 2–5 min, 90–10% B; 5–7 min, 5% B; 7–8 min, 90% B. The parameters of Mass spectrometry (MS) are as follows: electrospray voltage (ESI +, 5500 V), collision chamber inlet voltage (10.0 V), ion source temperature (550 ℃), auxiliary air pressure (50

psi), air curtain gas pressure (30 psi), atomization gas pressure (50 psi).

2.2. Preparation of AS/NZVI/GO nanocomposites

The dried AS was activated as follows: 10 g of AS was placed in an Erlenmeyer flask, 30 mL of 30% KOH was added and soaked for 30 min (Zhou et al., 2018b). Then activated AS was dried at 80 ℃ and then dried activated AS was milled to a fine powder.

The synthesis process mainly includes the following steps. 1) 4 g activated AS and 12 mL (1 mol*L^{-1}) $FeCl_3$ solution were added into an Erlenmeyer flask, and then the mixture was ultrasonicated for 2 h at room temperature. 2) the mixture was stirred for 12 h at 60 ℃ and was separated through vacuum filtration. 3) the residue was dried at 80 ℃ for 4 h through a vacuum drying oven. 4) the sample was heated from room temperature to final temperature (500, 600, 700 and 800 ℃) with a heating rate of 10 ℃ min^{-1} and hold for 120 min at a final temperature at N_2 atmosphere. 5) the sample was cooled inside the furnace, maintaining the N_2 atmosphere, and then washed with deionized water and ethanol more than three times. The resulting products were vacuum dried for use. In addition, in order to investigate the effect of the proportion of GO on the adsorption efficiency, adding 0, 10, 50 and 100 mL of GO solution with a concentration of 1000 mg·L^{-1} to the initial solution, and then those were pyrolyzed under the temperature of 700 ℃. The prepared samples were stored in sealed containers prior to use. The schematic illustration of the synthetic approach of the AS/NZVI/GO nanocomposites was shown in Fig. 1.

2.3. Characterization of AS/NZVI/GO nanocomposites

The morphology of adsorbent was investigated by a scanning electron microscope (SEM) (Quanta Q400, FEI Company, USA). Infrared spectrum (FT-IR) (IRTracer-100, Shimadzu, Japan) was utilized for the identification of the surface functional groups. Crystalline graphitic layer intensity and disordered carbon peaks of AS/NZVI/GO were confirmed by Raman. Surface elemental compositions were determined using an ESCALAB 250Xi X-ray photoelectron spectroscopy (XPS) (Thermo Fisher Scientific, USA). The magnetic property of the adsorbent was analyzed by a vibrating sample magnetometer (VSM) (MPMS (SQUID) XL-7, Quantum Design Co., USA) with the field cycling from −20 to 20 kOe at room temperature. The surface properties of the AS/NZVI/GO were investigated with N_2 adsorption–desorption measurement at 77 K using ASAP2460 (Micromeritics Company, USA). The Brunauer-Emmett-Teller (BET) method was used to calculate the specific surface areas (S_{BET}) (p/p^0 = 0.3). The total pore volume (V_T) was defined as the maximum volume of adsorbed at a relative pressure (p/p^0) of 0.99. The micropore volume (V_{micro}) was calculated using the t-Plot method. The mesopore volume was counted from the difference between the VT and Vmicro (VT - Vmicro). The average pore size was determined with the equation ($D_p = 4V_T/S_{BET}$). And the pore size distribution of various materials was obtained from the Horvath-Kawazoe method (Zhou et al., 2018b).

2.4. Adsorption experiments

The investigation of different pyrolysis temperatures and different GO ratios is as follows: 1) 10 mL of pesticide (10 mg·L^{-1}) and 10 mg of AS/NZVI/GO was added to the

Fig. 1 The procedure for the synthesis of AS/NZVI/GO and the process of pesticide adsorption.

flask, shaking for 30 min. 2) After AS/NZVI/GO adsorbs the pesticide molecules, it was separated from the solution with an external strong magnet. 3) the solution was transferred to 2 mL centrifuge tubes and followed by filtering with a 0.22 μm nylon filter. The control experiment was conducted under the same conditions without the AS/NZVI/GO. The whole adsorption process was performed at room temperature. The percentage of removal efficiency was calculated by the following formula (1) (Wang et al., 2020):

$$RE(\%) = (C_0 - C_e)/C_0 * 100\% \quad (1)$$

The adsorption capacity Q_e ($mg{\cdot}g^{-1}$) for pesticide was calculated by using Eq. (2):

$$Q_e = [(C_0 - C_e) * V]/W \quad (2)$$

where RE is the removal efficiency, C_0 ($mg{\cdot}L^{-1}$) is the initial pesticide concentration, and C_e ($mg{\cdot}L^{-1}$) is the pesticide concentration at equilibrium. V (L) is the volume of the pesticide solution. W (g) is the mass of AS/NZVI/GO.

The investigation of initial solution pH was as follows: the initial pH value was adjusted by adding a suitable amount of 0.1 $mol{*}L^{-1}$ HCl or NaOH. And the 0.01 $mol{*}L^{-1}$ NaCl was added to the solution to control ionic strength. The point of zero charge (pH_{PZC}) was determined and calculated by referring to the method of literature (Zhu et al., 2014).

2.4.1. Adsorption kinetic

The determination of adsorption kinetic was as follows: the adsorption kinetic tests were determined in a 50 mL flask containing 10 mg of adsorbents and 10 mL of the pesticide solution (50 $mg{\cdot}L^{-1}$), respectively. The aqueous samples were analyzed for 30 min at a regular interval. The model formulas of adsorption kinetics were as following (Zhang et al., 2021; Zhou et al., 2019):

$$\text{Pseudo-first-order (PFO) model}: Ln(Q_e - Q_t) = LnQ_e - K_1 t Ln(Q_e - Q_t) \quad (3)$$

$$\text{Pseudo-second-order (PSO) model}: t/Q_t = 1/K_2 Q_e^2 + t/Q_e \quad (4)$$

$$\text{Intra-particle diffusion (IPD) model}: Q_t = K_i t^{1/2} + C \quad (5)$$

$$\text{Liquid film diffusion (LFD) model}: Ln(1 - Q_t/Q_e) = -K_{fd} t + A \quad (6)$$

where Q_e and Q_t ($mg{\cdot}g^{-1}$) are removal amount of pesticides at equilibrium time and t time. K_1 (min^{-1}), K_2 ($g{\cdot}mg^{-1}{\cdot}min^{-1}$) and K_i ($mg{\cdot}g^{-1}{\cdot}\ min^{1/2}$) are the corresponding rate constants, t is the adsorption time, and C is the intercept represents the thickness of the boundary layer. The K_{fd} (min^{-1}) is the liquid film diffusion coefficient.

2.4.2. Adsorption isotherm

The determination of adsorption isotherm was as follows: different initial pesticides concentration solutions (4–50 $mg{\cdot}L^{-1}$ for Isoprocarb and 10–100 $mg{\cdot}L^{-1}$ for Methomyl and Carbaryl) were prepared to conduct the experiment, and then the samples were obtained at equilibrium time (30 min) and pesticides concentrations in the supernatant were determined. The model formulas of adsorption kinetics were as following (Zhang et al., 2021; Zhou et al., 2019):

$$\text{Langmuir model}: 1/Q_e = 1/Q_m K_L C_e^2 + 1/Q_m \quad (7)$$

$$\text{Freundlich model}: LnQ_e = LnK_F + 1/nC_e \quad (8)$$

$$\text{Temkin model}: Q_e = a\ LnK_T + a\ LnC_e \quad (9)$$

where Q_m ($mg{\cdot}g^{-1}$) is the maximum amount of adsorption corresponding to the monolayer coverage, Q_e ($mg{\cdot}g^{-1}$) is the amount of pesticides adsorbed at equilibrium and K_L ($L{\cdot}mg^{-1}$) is the Langmuir constant related to the adsorption energy. K_F ($mg{\cdot}g^{-1}$) is the adsorption capacity in the unit concentration, 1/n is the intensity of adsorption and C_e ($mg{\cdot}L^{-1}$) is the equilibrium concentration. The K_T ($L{\cdot}g^{-1}$) is the equilibrium bond constant related to the maximum energy of the bond.

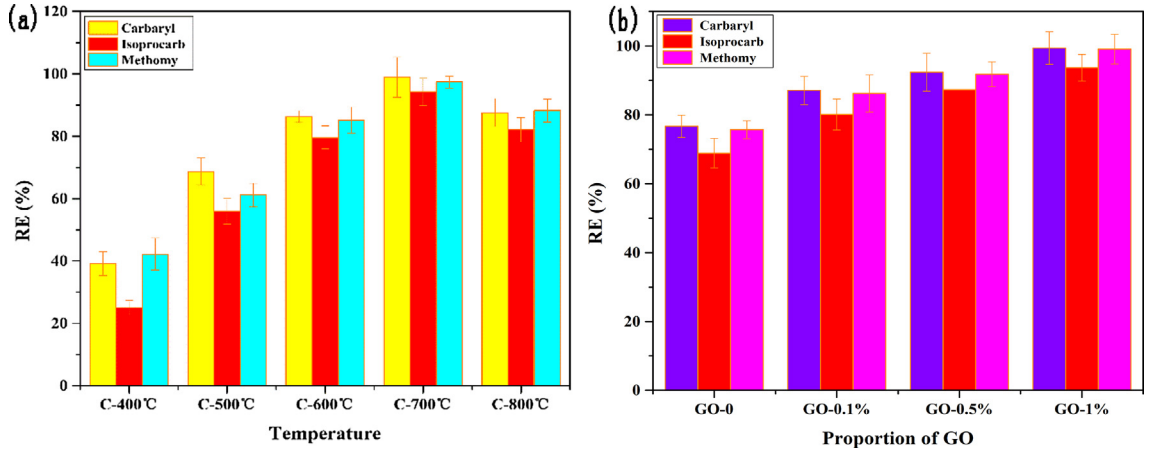

Fig. 2 (a) The effect of materials prepared at different pyrolysis temperatures on adsorption efficiency; (b) The effect of different GO additions on adsorption efficiency.

3. Result and discussion

3.1. Optimization of pyrolysis temperature and investigation of the proportion of GO

The pyrolysis temperature was a key factor affecting the expansion degree, pore size and structure of biochar, and its adsorption efficiency (Zhou et al., 2018a). In order to obtain the best adsorption efficiency, the pyrolysis temperature (500, 600, 700 and 800 ℃) was optimized. The result in Fig. 2a showed that the AS/NZVI/GO composite synthesized at the pyrolysis temperature of 700 ℃ has higher adsorption efficiency for pesticides than others. The reason might be explained that the AS/NZVI/GO-1% (700 ℃) has more pore structure or larger specific surface area to provide more adsorption sites for pesticide molecule than others. Therefore, 700 ℃ was selected as the optimal pyrolysis temperature. In addition, in order to select optimal GO addition amount, composite materials with 0–1% GO content were investigated. The result was shown in Fig. 2b. The result showed that the AS/NZVI/GO composite with 1% GO exhibited the best adsorption ability for the pesticides. Therefore, the 1% GO was selected as the optimal addition proportion for the synthetic composites.

3.2. Characteristics

The morphologies and microstructures of AS/NZVI/GO composite were investigated by SEM measurement (Fig. 3). According to Fig. 3a, a large number of pore structures could be observed. These pore structures could increase the specific surface area and porosity of the composite and further enhance adsorption efficiency. Meanwhile, it could be found that a small amount of sheet-like structure was attached to the surface of the material, which was considered to be GO (Fig. 3b). GO has a large number of aromatic structures, which could enhance the π-π interaction between pesticide molecules and composite material, and increase the adsorption efficiency for pesticides (Miao et al., 2019). In addition, it could be found that there were a lot of spherical particles on the surface of the material. The spherical particles were considered to be the magnetic NZVI particle. The composite combined by magnetic NZVI with biochar could quickly separate adsorbent and matrix after adsorbing the targets under the external magnetic

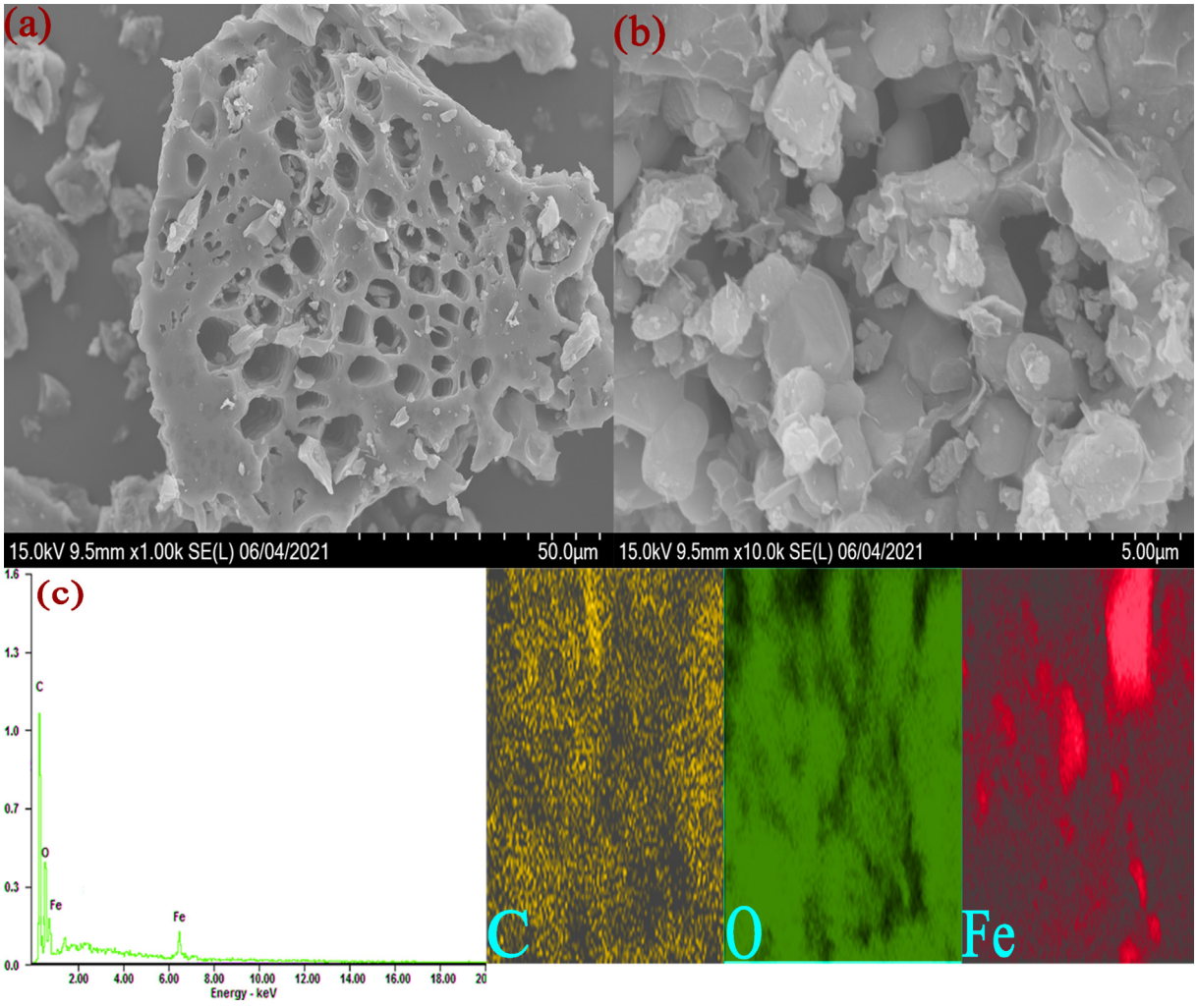

Fig. 3 (a) and (b) The SEM images of AS/NZVI/GO. (c) showed the result of EDS and element mapping.

field. The result of element mapping showed that the elements were evenly distributed in AS/NZVI/GO composite and the result of energy dispersive spectroscopy (EDS) showed that the C, O and Fe were well detected in the AS/NZVI/GO composite (Fig. 3c). The above results showed that AS/NZVI/GO composite was successfully prepared by combining the biochar, GO and NZVI.

The morphological characteristics of the AS/NZVI/GO composite (AS/NZVI/GO-500, AS/NZVI/GO-600, AS/NZVI/GO-700 and AS/NZVI/GO-800) were investigated by nitrogen adsorption isotherm. The characteristics include specific surface area, porosity and total pore volume, etc. As shown in Figure S1a, the isotherm of AS/NZVI/GO showed type I and type IV feature in accordance with the IUPAC (International Union of Pure and Applied Chemistry), which indicated that the material had a large number of microporous and mesoporous structures (Zhou et al., 2018b). Meanwhile, the result of the pore size distribution (Figure S1b) further proved AS/NZVI/GO composite possessed an abundance of micropores and mesopores. In addition, it was worth noting that AS/NZVI/GO-700 exhibited a higher adsorbed amount of nitrogen on AS/NZVI/GO compared with the ones prepared at other pyrolysis temperature. Furthermore, as could be seen from Table 1, AS/NZVI/GO-700 of average pore size was smaller than other materials and the specific surface of AS/NZVI/GO-700 was significantly higher than other materials. Those results further proved that the formation of pore structure was highly correlated with pyrolysis temperature, and also reflected the importance of pyrolysis temperature for the formation of high specific surface area and high porosity structure. At the same time, it further explained that the adsorption efficiency of AS/NZVI/GO-700 was the best.

In order to explore the structural characteristics of the AS/NZVI/GO composite material, Raman spectroscopy was applied. The results were shown in Figure S2. D band (1357 cm^{-1}) indicates the presence of disordered carbon or structure defects and G band (1606 cm^{-1}) confirms the stretching vibrations of sp^2 hybridized carbon atoms (Duman et al., 2021). The graphitic degree of AS/NZVI/GO was evaluated by the ID/IG value. The ID value corresponded to the peak area of the D band and the IG value corresponded to the peak area of the G band. In this study, the ID/IG value of AS/NZVI/GO-1% was 0.96, which showed that there were a lot of graphitized structures in the AS/NZVI/GO-1% composite material (Zhang et al., 2018a). Meanwhile, it could be found that the ID/IG value of AS/NZVI/GO-1% was slightly lower than the AS/NZVI without GO. The results further proved that the graphitic degree of bio-nanocomposites could be increased by increasing the content of GO, which was beneficial to the adsorption of pesticide molecules. It could further explain that AS/NZVI/GO-1% has better pesticide removal efficiency than other materials.

The surface groups of synthesized material were investigated by IR spectra in the range of 4000–400 cm^{-1}. The infrared spectra of AS/NZVI and AS/NZVI/GO-1% were shown in Figure S3. The absorption band was observed at 3483.41 cm^{-1}, which could correspond to the stretching vibration of the hydroxyl group (O-H). The absorption band at 2381.28 cm^{-1} could correspond to the carbon–carbon double bond structure in the benzene ring or aromatic ring (C = C). The absorption peak at 1091.51 cm^{-1} could correspond to the stretching vibration of the carbon–oxygen single bond (C–O). The absorption peak at 1613.42 cm^{-1} could correspond to the stretching vibration of the carbon–oxygen double bond (C = O) (Tang et al., 2020). These absorption bands further proved that the AS/NZVI/GO material contained a large number of hydroxyl groups, carbonyl groups, aromatic rings and other structures, which were related to the mechanism of adsorption of pesticide molecules (Zhou et al., 2020). In addition, it could be found that the absorption strength of each absorption band has increased to varying degrees, and the location of the stretching bands for the main functional groups was slightly shifted when the GO was introduced. The results further proved that GO was successfully synthesized onto the composite surface of the material, which could be concerned to be a potential adsorption site.

The chemical composition of AS/NZVI/GO was further investigated by XPS measurement. According to Figure S4a, it could be found that AS/NZVI/GO composite materials mainly contained the elements of Fe, O and C. According to the spectra of C1s in Figure S4b, the binding energy peaks at 284.15, 286.23, 288.37 and 283.84 eV could correspond to the C = C, C–C, C–O and C = O signals, respectively, which corresponds to the carbonyl, carboxyl, and aromatic structures on the surface of biochar materials and graphene oxide (Zhou et al., 2020). According to Figure S4c, the peaks at 532.19, 523.07 and 529.47 eV could correspond to the O–C, Fe–O, and C = O signals, respectively. The peaks around 720 eV could be assigned to iron oxides like FeO and FeOOH. The peak at 719 eV could be concerned with the existence of Fe^0 (Qi et al., 2020). Meanwhile, the magnetic performance of AS/NZVI/GO was measured by the VSM, and the result implied that it was sufficient enough for magnetic separation from the solution under the external magnetic field (Figure S5). In summary, it could be a drawn conclusion that AS/NZVI/GO was successfully synthesized in this work.

3.3. Effect of pH and investigation of the amount of adsorbent

The ionized form of the pesticide molecule in the solution and the existing form of the functional group on the surface of the adsorbent in the solution is mainly affected by the pH of the initial solution, which could further affect the adsorption process and adsorption efficiency (Deng et al., 2020). Thus, the

Table 1 The textural properties of AS/NZVI/GO synthesized at different temperatures (500℃, 600℃, 700℃ and 800℃).

Textural properties	AS/NZVI/GO-500	AS/NZVI/GO-600	AS/NZVI/GO-700	AS/NZVI/GO-800
S_{BET} - surface area ($m^2 \cdot g^{-1}$)	312	627	1157	942
V_T - total pore volume ($cm^3 \cdot g^{-1}$)	0.31	0.37	0.81	0.64
V_{micro} - micropore volume ($cm^3 \cdot g^{-1}$)	0.04	0.14	0.37	0.29
D_p - average pore diameter (nm)	6.43	4.32	3.09	3.41

initial solution pH (3–10) was investigated. The result was shown in Fig. 4a. It can be found that the removal rate was the highest when the pH was 7 and the removal rate was increased with the increase of pH (from 3 to 7), which indicated that the adsorption of the three pesticides onto the adsorbent was highly pH-dependent. The pH mainly affects the electrostatic interaction between adsorbent and adsorbate. The acid dissociation constants of methomyl, isoprocarb and carbaryl were pKa = 13.27 ± 0.46, pKa = 12.22 ± 0.46 and pKa = 12.02 ± 0.46, respectively. They mainly exist as protonated species at lower pH. Meanwhile, the surface charge of AS/NZVI/GO depends on the pH of the solution. The pHpzc of AS/NZVI/GO was 5.67 (Figure S10). The surface charge of the AS/NZVI/GO is rendered positive when the pH value is lower than pHpzc ($[AS/NZVI/GO]^+$). Therefore, the positively charged AS/NZVI/GO adsorbent and protonated pesticide molecules had electrostatic repulsion at lower pH, which led to the lower adsorption capacity. With the increase of pH, the surface charge of the AS/NZVI/GO is rendered negative when the pH value is greater than pHpzc ($[AS/NZVI/GO]^-$), and there was mainly electrostatic attraction between AS/NZVI/GO and pesticides molecule. However, it could be found that the removal rate was decreased rapidly when the pH value was greater than 8. The reason was that the three pesticide molecules were quickly decomposed when the solution is alkaline (Wang et al., 2020). In summary, pH = 7 was selected as the optimal experimental condition for this experiment.

In addition, the amount of adsorbent was considered to be an important factor to affecting its adsorption efficiency. Thus, in order to obtain the best adsorption efficiency, the amount of adsorbent (4–20 mg) was investigated. The results showed that the removal rate of three pesticides was increased as the amount of adsorbent increases. And the pesticides were almost completely adsorbed when the amount of adsorbent was 10 mg (Fig. 4b). Therefore, 10 mg was selected as the optimal amount of adsorbent.

3.4. Adsorption kinetic

Adsorption kinetics is usually used for describing the relationship between the mass transfer and time of the adsorbate during the adsorption process, to explain its adsorption process and adsorption efficiency. At first, the pseudo-first-order kinetic model (PFO) and pseudo-second-order kinetic model (PSO) was used to fit the data of this experiment. In the current study, the adsorption kinetics curves were shown in Figure S6 and the experimental data of removal and fitting parameters for three pesticides were shown in Table 2. According to Figure S6, it could be found that the adsorption process was divided into three steps, which included fast adsorption, slow adsorption and dynamic equilibrium stage. According to Table 2, it could be found that the correlation coefficient value (R^2) of the PFO model was lower than the PSO model. Meanwhile, it could be seen that Q_e values calculated by the PSO model were closer to the experimental Q_e values. The above results confirmed that the PSO model was more suitable for describing the adsorption process of three pesticides on AS/NZVI/GO composite. At the same time, it indicated that the adsorption process between the AS/NZVI/GO composite and the pesticide (Table 3a) involves the chemical interaction of electron transfer (Zhou et al., 2019).

In addition, to further understand the mechanism and rate control steps affecting the adsorption kinetics, the adsorption process was studied by the intra-particle diffusion model (IPD) and liquid film diffusion model (LFD). According to the LFD model (Figure S7 and Table 3a,b), it could be found that the R^2 values were greater than 0.98 and the intercept was almost zero (K_{fd} values), which indicated the diffusion of pesticide molecules in the boundary liquid film around the composite was one of the steps that limit the adsorption rate (Javadian et al., 2015). In addition, it could be seen that the plot of the IPD model included three linear steps, which indicated that the adsorption process consists of three stages (Figure S8). The first stage was corresponding to the surface diffusion controlled by membrane diffusion, and the second stage was corresponding to the membrane diffusion and intra-granular diffusion, and the third stage was corresponding to adsorption equilibrium. The slope of the first stage was greater than the second stage ($k_1 > k_2$), which could be interpreted as follows: on the one hand, there was a high concentration difference in the adsorbate at the interface between the AS/NZVI/GO composite and the solution, thus a strong mass driving force was generated. It promotes the adsorbate to be

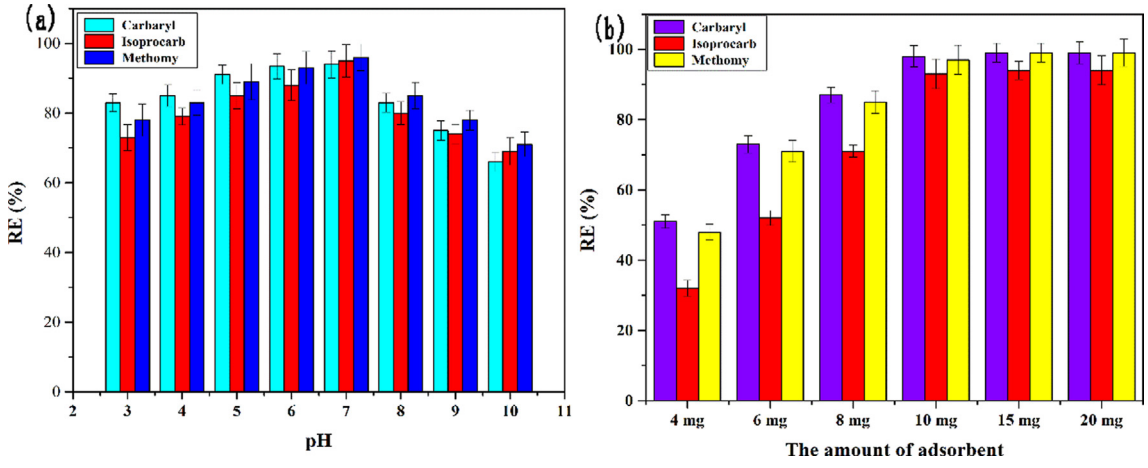

Fig. 4 (a) The effect of different initial solution pH on the efficiency of pesticide adsorption. (b) The investigation of the amount of adsorbent of the AS/NZVI/GO.

Table 2 Parameters of the pseudo-first-order and pseudo-second-order adsorption kinetic models for the adsorption of pesticides onto AS/NZVI/GO.

Pesticides	Q_e (exp) ($mg \cdot g^{-1}$)	pseudo-first-order kinetic model			pseudo-second order kinetic model		
		Q_e ($mg \cdot g^{-1}$)	K_1 (min^{-1})	R^2	Q_e ($mg \cdot g^{-1}$)	K_2 ($g \cdot mg^{-1} \cdot min^{-1}$)	R^2
Methomyl	35.97	49.78	0.134	0.982	38.92	0.0026	0.994
Isoprocarb	15.23	20.43	0.146	0.964	16.07	0.0069	0.984
Carbaryl	40.31	55.17	0.133	0.978	42.83	0.0023	0.991

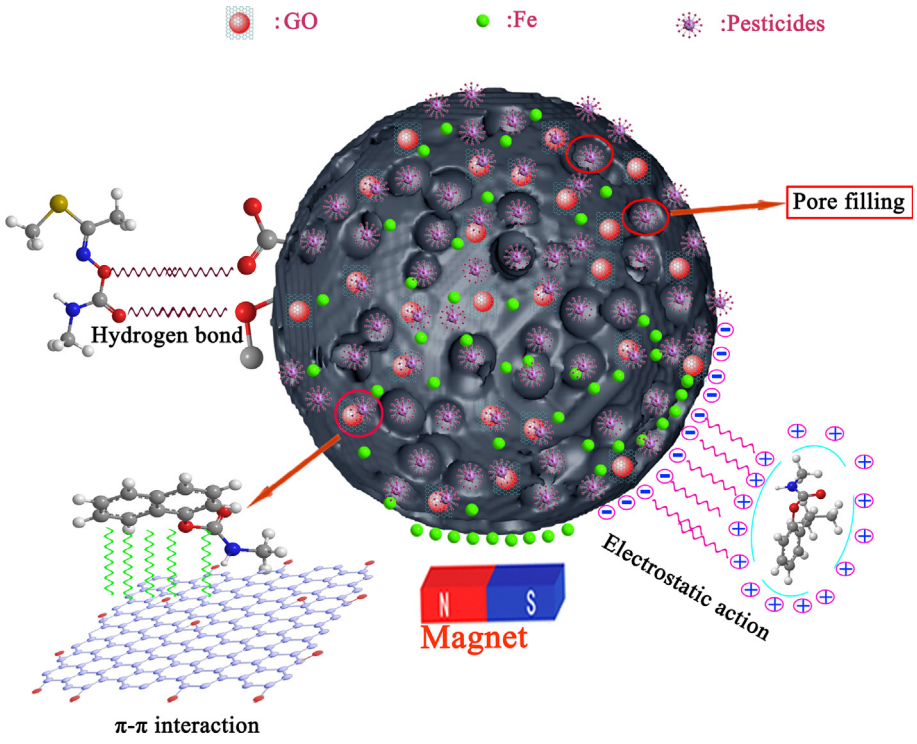

Fig. 5 The schematic diagram of the possible adsorption mechanism of AS/NZVI/GO on pesticide molecules.

Table 3a Parameters of the liquid film diffusion model for the adsorption of pesticides onto AS/NZVI/GO.

Liquid film diffusion model			
Pesticides	Methomyl	Isoprocarb	Carbaryl
K_{fd} (min^{-1})	−0.1345	−0.1461	−0.1336
A	38.92	16.07	42.83
R^2	0.994	0.984	0.992

Table 3b Parameters of intra-particle diffusion model for the adsorption of pesticides onto AS/NZVI/GO.

Intra-particle diffusion model			
Pesticides	Methomyl	Isoprocarb	Carbaryl
K_{i1} ($mg \cdot g^{-1} \cdot min^{1/2}$)	6.28	3.02	7.29
C_1 ($mg \cdot g^{-1}$)	1.65	2.56	0.62
R_{i1}^2	0.997	0.998	0.984
K_{i2} ($mg \cdot g^{-1} \cdot min^{1/2}$)	2.417	0.7578	2.631
C_2 ($mg \cdot g^{-1}$)	16.72	8.97	18.49
R_{i2}^2	0.974	0.980	0.968
K_{i3} ($mg \cdot g^{-1} \cdot min^{1/2}$)	0.1769	0.0397	0.1616
C_3 ($mg \cdot g^{-1}$)	34.59	14.75	38.41
R_{i3}^2	0.987	0.985	0.987

transferred to the surface of the AS/NZVI/GO composite through the liquid film, which could accelerate the adsorption rate. On the other hand, the adsorption sites decrease and internal diffusion resistance increases could slightly slow down the adsorption rate (Ahmed et al., 2016). The results of IPD showed that the diffusion of pesticide molecules from the surface of the AS/NZVI/GO composite to its internal structure was also one of the main rate-limiting steps. Besides, the fitting line did not pass the (0, 0) point of the coordinate system, which indicated that there were other rate-determinants in the adsorption process other than IPD (Yu et al., 2020).

3.5. Adsorption isotherm studies

The adsorption isotherm model is also considered to be an effective method for describing the interaction between adsorbent and adsorbate, such as Langmuir, Freundlich and Temkin isotherm models (Zhang et al., 2021). In the current study, the results of three adsorption isotherm models fitted were shown in Figure S9 and Table 4. According to the results, it could be found that the Freundlich isotherm model was considered more suitable for fitting this adsorption process because the R^2 value being much closer to 1.0 compared to that of the other models, which indicated that the adsorption process by which the AS/NZVI/GO adsorbs pesticide molecules was mainly limited by the multimolecular layer chemical and physical adsorption with ion sharing and transferring. The obtained adsorption isotherm model results are consistent with the previous studies conducted for various adsorbent-pollutant systems (Duman & Ayranci, 2005). Meanwhile, the result of $1/n > 1$ showed that there was a positive cooperative effect between the three pesticides in binding with the AS/NZVI/GO (Yu et al., 2020). The correlation coefficient of the Temkin adsorption isotherm model was 0.942. The result indicated that the energy change of the adsorption of pesticides on AS/NZVI/GO was affected by temperature and electrostatic interaction occurred throughout the process (Jang et al., 2018). Meanwhile, the results of the Langmuir isotherm model fitting showed that the adsorption capacity of the AS/NZVI/GO for the three pesticides was significantly different. The maximum adsorption capacity of three pesticides methomyl, isoprocarb and carbaryl were 59.13, 21.33 and 61.91 mg g^{-1}, respectively.

3.6. Adsorption mechanism

In general, the pesticide adsorption process could be summarized as a multi-step process. It mainly included that the pesticide molecules diffuse from the solution phase to the surface of the adsorbent, and then from the surface of the adsorbent to the internal or external pore structure, and firmly bind to its active site. The adsorption mechanism of pesticides on AS/NZVI/GO composite was shown in Fig. 5. And it mainly included electrostatic interaction, pore filling, hydrogen bonding force, π-π interaction and hydrophobic interaction, etc. (Dai et al., 2020). The pH experiment results showed that there was electrostatic interaction between the AS/NZVI/GO composite and the pesticide molecule. The results of BET confirmed that the AS/NZVI/GO composite had a rich porous structure, which contributed to the diffusion of the pesticide molecular into the internal surface of the adsorbent. Besides, the hydrogen bond interactions might be formed between pesticide molecular and oxygen-containing functional groups on the surface of the AS/NZVI/GO composite, which was considered an important driving force for pesticide adsorption (Nodeh et al., 2019). Meanwhile, the strong π-π stacking interaction might contribute to the pesticide adsorption due to the presence of the graphite structure and aromatic rings in AS/NZVI/GO composite (Dai et al., 2020; Zhang et al., 2020). By comparing the Raman spectrum of the AS/NZVI/GO composite before and after adsorption (Figure S2), it could be found that the G band shifted from 1606 cm^{-1} to 1619 cm^{-1}. It could be explained that the adsorption of pesticide molecules may be through the formation of π-π interaction with the AS/NZVI/GO composite material, and causing the Raman spectrum to shift. Thus, the above results further confirmed that there was a π-π interaction between the pesticide molecular and the AS/NZVI/GO composite (Zhang et al., 2018a). To sum up, the electrostatic interaction, pore filling, hydrogen bonding force, π-π interaction and hydrophobic interaction might be the mechanism by which pesticide molecules were adsorbed by AS/NZVI/GO.

3.7. Analysis of real samples

In order to examine the removal capacity of the AS/NZVI/GO for pesticides in a real sewage sample, the sewage collected in the sewage tank was used as a real sample in the following experiment. 10 mL pesticide standards (10 mg·L^{-1}) were added to the sewage samples. And then 10 mg AS/NZVI/GO was used to absorb the pesticides. Then the removal rate was determined. The removal rate for Methomyl, Isoprocarb and Carbaryl was 97.24%, 93.41% and 96.92%, respectively, which indicated that the AS/NZVI/GO had a good adsorption effect on pesticides in sewage.

3.8. Reusability of adsorbents

In addition, to explore the reusability of AS/NZVI/GO composite for pesticide adsorption, 0.1 mol*L^{-1} NaOH solution was used as an eluant to carry out the recycling experiment. After five recycles, the AS/NZVI/GO composite still hold good reusable adsorption property (77.51%, 72.42% and 74.51% removal efficiency, respectively) (Fig. 6). The good regeneration indicated that AS/NZVI/GO composite was a promising adsorbent with excellent reusability and stability.

Table 4 Parameters of the Freundlich, Temkin and Langmuir isotherm model for the adsorption of pesticides onto AS/NZVI/GO.

	Pesticides	Methomyl	Isoprocarb	Carbaryl
Freundlich isotherm model	K_F (mg·g^{-1})	0.01257	0.1039	0.00642
	R^2	0.993	0.989	0.991
	1/n	4.46	3.59	5.02
Temkin model	K_T (L·g^{-1})	15.8304	5.3362	16.9860
	R^2	0.983	0.903	0.968
	a	0.177	0.595	0.178
Langmuir isotherm model	Q_m (mg·g^{-1})	59.13	21.33	61.91
	R^2	0.983	0.975	0.982
	K_L (L·g^{-1})	0.00504	0.02013	0.00356

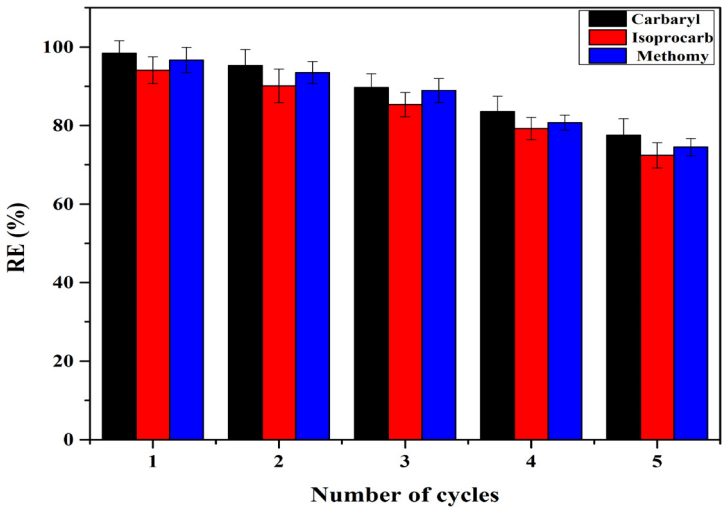

Fig. 6 The removal efficiency of AS/NZVI/GO to pesticide after a continuous 5 regeneration cycle.

3.9. Comparison with other adsorbents

The comparison with other adsorbents used for removal or adsorb pesticides was summarized in Table S1. It could be found that the AS/NZVI/GO composite exhibited high adsorption capacity when adsorbing three pesticides simultaneously. Meanwhile, comparing to the other adsorbents, the novel AS/NZVI/GO composite had potential advantages. On the one hand, the AS/NZVI/GO composite could be quickly separated from the matrix after adsorbing the target. On the other hand, the synthesis and use process of AS/NZVI/GO composite were environmentally friendly and no harmful reagents were used. At the same time, the synthesis was simple and suitable for batch operation. It was synthesized using a one-step synthesis method. Furthermore, the AS/NZVI/GO composite had excellent regeneration performance. Those proved that the AS/NZVI/GO composite was an economical, environmentally friendly and efficient pesticide adsorbent.

4. Conclusions

In the study, the novel magnetic nanoporous carbon composite was successfully synthesized by one-step pyrolysis through combining nano-zero-valent iron, Angelicae Dahuricae Radix waste and graphene oxide, and it displayed high removal efficiency for pesticides and the maximum adsorption capacity for methomyl, isoprocarb and carbaryl reached 59.13, 21.33 and 61.91 $mg{\cdot}g^{-1}$, respectively, as well as the removal efficiency could reach more than 70% after five recycles.

Meanwhile, the results of the characterization including SEM, BET, FTIR, XPS, VSM and Raman) showed the AS/NZVI/GO had abundant pore structures, surface functional groups and high specific surface area, which could enhance the adsorption efficiency. Furthermore, the factors that have a significant impact on adsorption efficiency, including solution pH, pyrolysis temperature of biochar and proportion of GO, were investigated. The results exhibited that the removal rate was the highest when the pH was 7 and the pyrolysis temperature and proportion of GO were 700 ℃ and 1%, respectively. In addition, the results of adsorption kinetics and isotherms models indicated that experimental data for AS/NZVI/GO could be well fitted by the PSO and Freundlich isotherm model. In summary, it could be concluded that the prepared AS/NZVI/GO was an economical, environmentally friendly and efficient adsorbent for removing pesticides from sewage.

CRediT authorship contribution statement

Hua Du designed and carried out experiments and wrote the manuscript. Yutian Lei and Wenli Chen completed drawing and analyzed experimental results. Fengchao Li, Huimin Li and Wei Deng analyzed experimental results. Guihua Jiang directed the experiment and assisted with the writing of the manuscript.

Declaration of Competing Interest

The authors declare that they have no known competing financial interests or personal relationships that could have appeared to influence the work reported in this paper.

Acknowledgments

This work is supported by the major research and development project of the Ministry of Science and Technology: Research on the appropriate technology and industrialization model of ethnic medicine resource regeneration and ecological protection (No. 2019YFC1712305). Sichuan Provincial Department of Science and Technology Application Basic Project: Research on Rapid Detection Technology of Sulfur Dioxide Limit Based on Baizhi Scientific Sulphur Fumigation Technology (No. 2020YJ0369).

Appendix A. Supplementary material

Supplementary data to this article can be found online at https://doi.org/10.1016/j.arabjc.2021.103267.

References

Ahmed, S.M. et al, 2016. A kinetic study for the removal of anionic sulphonated dye from aqueous solution using nano-polyaniline and Baker's yeast. Arabian J. Chem. 9, S1721–S1728.

Al-Marghany, A. et al, 2021. Fabrication of Schiffâ0080™s base-functionalized porous carbon materials for the effective removal of toxic metals from wastewater. Arabian J. Geosci. 14 (5), 336.

Alothman, Z.A. et al, 2020a. Fabrication of renewable palm-pruning leaves based nano-composite for remediation of heavy metals pollution. Arabian J. Chem. 13 (4), 4936–4944.
Alothman, Z.A. et al, 2020b. Development of combined-supramolecular microextraction with ultra-performance liquid chromatography-tandem mass spectrometry procedures for ultra-trace analysis of carbaryl in water, fruits and vegetables. Int. J. Environ. Anal. Chem., 1–11
Bucur, M.P. et al, 2014. In vitro investigation of anticholinesterase activity of four biochemical pesticides: spinosad, pyrethrum, neem bark extract and veratrine. J. Pesticide Sci. 39 (1), 48–52.
Dai, J. et al, 2020. Effects of modification and magnetization of rice straw derived biochar on adsorption of tetracycline from water. Bioresour. Technol. 311, 123455.
Deng, J. et al, 2020. Different adsorption behaviors and mechanisms of a novel amino-functionalized hydrothermal biochar for hexavalent chromium and pentavalent antimony. Bioresour. Technol. 310, 123438.
Duman, O. et al, 2019. Carbon nanotube-based magnetic and non-magnetic adsorbents for the high-efficiency removal of diquat dibromide herbicide from water: OMWCNT, OMWCNT-Fe3O4 and OMWCNT-Îş-carrageenan-Fe3O4 nanocomposites. Environ. Pollut. 244, 723–732.
Duman, O., Ayranci, E., 2005. Structural and ionization effects on the adsorption behaviors of some anilinic compounds from aqueous solution onto high-area carbon-cloth. J. Hazard. Mater. 120 (1), 173–181.
Duman, O. et al, 2021. Development of highly hydrophobic and superoleophilic fluoro organothiol-coated carbonized melamine sponge/rGO composite absorbent material for the efficient and selective absorption of oily substances from aqueous environments. J. Environ. Chem. Eng. 9, (2) 105093.
Duman, O. et al, 2016. Removal of triphenylmethane and reactive azo dyes from aqueous solution by magnetic carbon nanotube-Îş-carrageenan-Fe3O4 nanocomposite. J. Alloy. Compd. 687, 370–383.
Duman, O. et al, 2017. Corrigendum to Synthesis of magnetic oxidized multiwalled carbon nanotube-Îş-carrageenan-Fe3O4 nanocomposite adsorbent and its application in cationic Methylene Blue dye adsorption. Carbohydr. Polym. 163, 338.
Gu, Y. et al, 2020. Lignosulfonate functionalized g-C3N4/carbonized wood sponge for highly efficient heavy metal ion scavenging. J. Mater. Chem. A 8 (25).
Habila, M.A. et al, 2018. Activated carbon cloth filled pipette tip for solid phase extraction of nickel(II), lead(II), cadmium(II), copper (II) and cobalt(II) as 1,3,4-thiadiazole-2,5-dithiol chelates for ultra-trace detection by FAAS. Int. J. Environ. Anal. Chem. 98 (2), 171–181.
Jang, H.M. et al, 2018. Adsorption isotherm, kinetic modeling and mechanism of tetracycline on Pinus taeda-derived activated biochar. Bioresour. Technol. 259, 24–31.
Javadian, H. et al, 2015. Study of the adsorption of Cd (II) from aqueous solution using zeolite-based geopolymer, synthesized from coal fly ash; kinetic, isotherm and thermodynamic studies. Arabian J. Chem. 8 (6), 837–849.
Jiang, S. et al, 2017. Adsorption of procyanidins onto chitosan-modified porous rice starch. LWT, 10–17.
Li, Z. et al, 2017. Highly efficient removal of chlorotetracycline from aqueous solution using graphene oxide/TiO2 composite: Properties and mechanism. Appl. Surf. Sci. 425 (dec.15), 765–775.
Markus, A. et al, 2018. Magnetite-sporopollenin/graphene oxide as new preconcentration adsorbent for removal of polar organophosphorus pesticides in vegetables. Environ. Sci. Pollut. Res.
Miao, J. et al, 2019. The adsorption performance of tetracyclines on magnetic graphene oxide: A novel antibiotics absorbent. Appl. Surf. Sci. 475 (MAY 1), 549–558.
Nodeh, H.R. et al, 2019. Equilibrium, kinetic and thermodynamic study of pesticides removal from water using novel glucamine-calix [4]arene functionalized magnetic graphene oxide. Environ. Sci.-Process. Imp. 21 (4), 714–726.
Nouri, N. et al, 2020. Overview of nanosorbents used in solid phase extraction techniques for the monitoring of emerging organic contaminants in water and wastewater samples. Trends Environ. Anal. Chem. 25, e00081.
Olu-Owolabi, B.I. et al, 2017. Adsorptive removal of 2,4,6-trichlorophenol in aqueous solution using calcined kaolinite-biomass composites. J. Environ. Manage. 192 (MAY1), 94–99.
Qi, Z.A. et al, 2020. Active biochar support nano zero-valent iron for efficient removal of U(VI) from sewage water. J. Alloy. Compd. 852.
Sereshti, H. et al, 2020. Nanosorbent-based solid phase microextraction techniques for the monitoring of emerging organic contaminants in water and wastewater samples. Microchim. Acta 187 (9), 541.
Shi, J. et al, 2016. Synthesis of graphene encapsulated Fe3C in carbon nanotubes from biomass and its catalysis application. Carbon 99, 330–337.
Shu, H., et al., 2018. Hybrid-type carbon microcoil-chitosan composite for selective extraction of aristolochic acid I from Aristolochiaceae medicinal plants. J. Chromatogr. A, 1561, 13–19.
Subedi, N. et al, 2019. A comparative study of magnetic chitosan (Chi@Fe3O4) and graphene oxide modified magnetic chitosan (Chi@Fe3O4GO) nanocomposites for efficient removal of Cr(VI) from water. Int. J. Biol. Macromol. 137, 948–959.
Sun, Q. et al, 2018. Pristine and modified radix Angelicae dahuricae (Baizhi) residue for the adsorption of methylene blue from aqueous solution: A comparative study. J. Mol. Liq. 265, 36–45.
Tang, T. et al, 2020. Chitosan functionalized magnetic graphene oxide nanocomposite for the sensitive and effective determination of alkaloids in hotpot. Int. J. Biol. Macromol. 146, 343–352.
Wang, Y. et al, 2020. Activated carbon derived from waste tangerine seed for the high-performance adsorption of carbamate pesticides from water and plant. Bioresour. Technol. 316, 123929.
Yadav, S. et al, 2019. Graphene Oxide as Proficient Adsorbent for the Removal of Harmful Pesticides: Comprehensive Experimental Cum DFT Investigations. Anal. Chem. Lett. 9 (3), 291–310.
Yu, Y. et al, 2020. Unraveling sorption of Cr (VI) from aqueous solution by FeCl3 and ZnCl2-modified corn stalks biochar: Implicit mechanism and application. Bioresour. Technol. 297, 122466.
Zhang, et al., 2018. Characterization of biochar derived from rice husks and its potential in chlorobenzene degradation. Carbon Int. J. (Sponsored by the American Carbon Society).
Zhang, et al., 2018. Biomass chitosan derived cobalt/nitrogen doped carbon nanotubes for the electrocatalytic oxygen reduction reaction. J. Mater. Chem. A Mater. Energy Sustain.
Zhang, P. et al, 2021. Characteristics, adsorption behaviors, Cu(II) adsorption mechanisms by cow manure biochar derived at various pyrolysis temperatures. Bioresour. Technol. 331, 125013.
Zhang, W. et al, 2019. Preparation, Mechanical Properties, and Biocompatibility of Graphene Oxide-Reinforced Chitin Monofilament Absorbable Surgical Sutures. Mar. Drugs 17 (4).
Zhang, Y. et al, 2020. Radix Astragali and Radix Angelicae Sinensis in the Treatment of Idiopathic Pulmonary Fibrosis: A Systematic Review and Meta-analysis. Front. Pharmacol. 11.
Zhao, T. et al, 2018. Facile low-temperature one-step synthesis of pomelo peel biochar under air atmosphere and its adsorption behaviors for Ag(I) and Pb(II). Sci. Total Environ. 640–641, 73–79.
Zhou, Y. et al, 2018a. Cost-efficient magnetic nanoporous carbon derived from citrus peel for the selective adsorption of seven insecticides. J. Sep. Sci. 41 (14).
Zhou, Y. et al, 2018b. Controllable synthesis of magnetic nanoporous carbon with tunable porosity for the efficient cleanup of vegetable samples. Anal. Chim. Acta 1041, 58–67.
Zhou, Y. et al, 2019. A novel Fe3O4/graphene oxide/citrus peel-derived bio-char based nanocomposite with enhanced adsorption

affinity and sensitivity of ciprofloxacin and sparfloxacin. Bioresour. Technol. 292, 121951.
Zhou, Y. et al, 2020. A three dimension magnetic bio-char composite-based quick, easy, cheap, effective, rugged and safe method for multi-pesticides analysis of vegetables. J. Chromatogr. A 1615, 460770.
Zhu, F. et al, 2017. Green synthesis of nano zero-valent iron/Cu by green tea to remove hexavalent chromium from groundwater. J. Cleaner Prod. 174 (FEB.10), 184–190.
Zhou, K., Ma, W., Zeng, Z., chen, R., Xu, X., Liu, B., Li, H., Li, H., Li, L., 2020. Waste biomass-derived oxygen and nitrogen co-doped porous carbon/MgO composites as superior acetone adsorbent: Experimental and DFT study on the adsorption behavior. Chemical Engineering Journal 387.
Zhu, H. et al, 2009. Removal of arsenic from water by supported nano zero-valent iron on activated carbon. J. Hazard. Mater. 172 (2–3), 1591–1596.
Zhu, X. et al, 2014. Preparation of magnetic porous carbon from waste hydrochar by simultaneous activation and magnetization for tetracycline removal. Bioresour. Technol. 154, 209–214.
Zubir, N.A. et al, 2014. Structural and functional investigation of graphene oxide-Fe3O4 nanocomposites for the heterogeneous Fenton-like reaction. Sci. Rep. 4, 4594.